

Effect of apical oxygen replacement by chlorine on the thermodynamic properties of $\text{Ca}_{1.82}\text{Na}_{0.18}\text{CuO}_2\text{Cl}_2$ single crystals

Kyung-Hee Kim,¹ Heon-Jung Kim,¹ Jung-Dae Kim,¹ H.-G. Lee,¹ and Sung-Ik Lee^{1,2}

¹National Creative Research Initiative Center for Superconductivity and Department of Physics, Pohang University of Science and Technology, Pohang 790-784, Republic of Korea

²Quantum Material Laboratory, Korea Basic Science Institute, Daejeon 305-333, Korea

(Received 18 June 2005; revised manuscript received 5 October 2005; published 15 December 2005)

We report the reversible magnetization of the $\text{Ca}_{2-x}\text{Na}_x\text{CuO}_2\text{Cl}_2$ ($x=0.18$) single crystal for $H\parallel c$ up to 1.2 T to study the effect of oxygen replacement by chlorine at the apical site. The superconducting transition temperature T_c (~ 27 K) of this single crystal is the highest reported in this family. Various thermodynamic parameters, such as the penetration depth $\lambda_{ab}(0)$, the coherence length $\xi_{ab}(0)$, the critical field $H_c(0)$, the upper critical field $H_{c2}(0)$ and the Ginzburg-Landau parameter κ , are also reported. Compared to the iso-structural compound $\text{La}_{1.82}\text{Sr}_{0.18}\text{CuO}_4$ with apical oxygen, $\text{Ca}_{1.82}\text{Na}_{0.18}\text{CuO}_2\text{Cl}_2$ has two significant differences: (1) $\lambda_{ab}(0)$ is larger, so the Cooper pair density is quite reduced, and (2) the anisotropic nature is more enhanced. From these observations, chlorine at the apical site is thought to be less effective than oxygen in supplying charge carriers to the CuO_2 planes; as a result, the interlayer coupling between the CuO_2 planes is weakened.

DOI: [10.1103/PhysRevB.72.224510](https://doi.org/10.1103/PhysRevB.72.224510)

PACS number(s): 74.72.Jt, 74.25.Bt

I. INTRODUCTION

The cuprate superconductor of oxychloride $\text{Ca}_{2-x}\text{Na}_x\text{CuO}_2\text{Cl}_2$ (Ref. 1) (hereafter called Na-CCOC) has attracted great attention for three reasons. First, it is a very good material for studying the role of apical oxygens. Second, single crystals are available over a wide range of the underdoped region. Third, the Na-CCOC single crystal is regarded as an ideal material for angle-resolved photoemission spectroscopy (ARPES) or scanning tunnelling microscopy (STM), both of which require highly clean surface. Moreover, Na-CCOC single crystals are cleaved as easily as $\text{Bi}_2\text{Sr}_2\text{CaCu}_2\text{O}_{8+x}$ (Bi-2212) single crystals, and Na-CCOC is free from the modulation and the orthorhombic distortion suffered by Bi-2212 and $\text{La}_{2-x}\text{Sr}_x\text{CuO}_4$ (LSCO),² respectively.

One major drawback of Na-CCOC is the extreme difficulty in synthesizing single crystals. Several GPa of high pressure are needed to grow the single crystals. Furthermore, the pressure must be carefully controlled to obtain the desired doping state of the crystal. It should be noted that the maximum T_c of previously synthesized single crystals is 21 K.⁷ Another drawback is that this compound is highly hygroscopic and so special attention must be paid so as not to expose the sample to air.

Structurally, Na-CCOC is very similar to LSCO and has a simple tetragonal K_2NiF_4 -type structure with one single CuO_2 plane per primitive cell. The only difference is that the oxygen atoms at the apices of the CuO_6 octahedra in LSCO are replaced by chlorine in Na-CCOC.

Recently, the results of ARPES and STM measurements on Na-CCOC single crystals have been reported and provided important insights to the mechanism of the cuprate superconductors. The STM study³ showed that for $|E| \leq 100$ meV, states within the gap undergo a clear “checkerboard” pattern of intense conductance modulations with a four-unit-cell ($4a_0$) periodicity. Such a behavior has been

similarly observed in underdoped Bi-2212.⁴ These results suggest that the checkerboard state can be a candidate of a hidden electronic order associated with the copper-oxide pseudogap. The ARPES measurements on Na-CCOC found two different gaps, a very small one contributing to the nodal region and a very large one dominating the antinodal region. Especially, the latter was found to result from an electronic structure typically seen in an undoped antiferromagnetic insulator.^{5,6} In addition, an interesting phenomenon, a “chemical potential shift” to the top of the valence band, was observed when the insulator $\text{Ca}_2\text{CuO}_2\text{Cl}_2$ was doped with Na.^{6,7} This is in contrast to the prevailing idea of a “pinned chemical potential,” which was inferred from experiments in $\text{La}_{2-x}\text{Sr}_x\text{CuO}_4$.⁸

Even though the physics of this compound is extremely interesting, not many experiments, other than the above two experiments, have been performed. The basic superconducting parameters, such as the upper critical field $H_{c2}(T)$, the penetration depth $\lambda_{ab}(0)$, the coherence length $\xi_{ab}(0)$, and the Ginzburg-Landau parameter $\kappa(T)$, have not been determined yet. This is partly because of the complicated and delicate synthesis condition of the single crystals. However, we successfully synthesized $\text{Ca}_{2-x}\text{Na}_x\text{CuO}_2\text{Cl}_2$ single crystal with $T_c=27$ K. This superconducting T_c is the highest reported so far for this compound, and from a comparison with polycrystalline samples, this doping state of the Na-CCOC compound is believed to be the optimal one with $x \approx 0.18$.^{1,9} The synthesis of single crystals with less doping is also possible with our setup.

In this paper, we present the reversible magnetization of the $\text{Ca}_{1.82}\text{Na}_{0.18}\text{CuO}_2\text{Cl}_2$ single crystal for magnetic fields applied parallel to the c axis. The basic superconducting parameters mentioned above were obtained. Unexpectedly, compared to the properties of $\text{La}_{1.82}\text{Sr}_{0.18}\text{CuO}_4$ with the same structure, those of $\text{Ca}_{1.82}\text{Na}_{0.18}\text{CuO}_2\text{Cl}_2$ are quite unusual. For example, the penetration depth $\lambda_{ab}(0)$, which contains information on the charge carrier density in the CuO_2 planes,

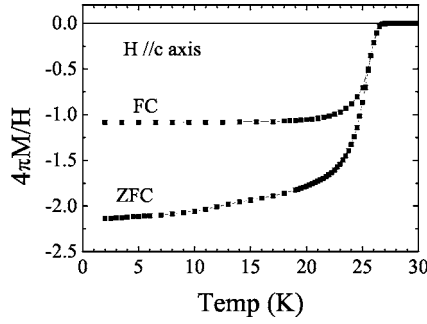


FIG. 1. Temperature dependence of the field-cooled (FC) and the zero-field-cooled (ZFC) magnetization, $4\pi M(T)$, for $H=10$ Oe parallel to c axis.

is larger than that of $\text{La}_{1.82}\text{Sr}_{0.18}\text{CuO}_4$. Also, by using the scaling theory¹⁰ and an analysis of irreversibility field H_{irr} , we found that two-dimensional (2D) nature was pronounced for Na-CCOC. From these observations, we deduced that the interlayer coupling in Na-CCOC was reduced.

II. EXPERIMENT

Single crystals of Na-CCOC were prepared by using a flux method in a high-pressure condition with the precursors $\text{Ca}_2\text{CuO}_2\text{Cl}_2$, NaClO_4 , and NaCl . The precursor $\text{Ca}_2\text{CuO}_2\text{Cl}_2$ was prepared at ambient pressure from the powders Ca_2CuO_3 , CuO , and CuCl_2 with 99.99% purities. Na was supplied from NaClO_4 and NaCl . The mixture of these powders were placed in a Pt capsule and pressed almost isostatically up to 5.2 GPa. The temperature was ramped to 1150–1200 °C in 30 minutes, kept stable for 1 h, and then slowly decreased to 750–850 °C. The obtained single crystals typically had sub-millimeter sizes.

A shiny and flat single crystal with dimensions of $1 \times 1 \times 0.3$ mm³ was used for the magnetization measurements. Before these measurements, this single crystal was characterized by using x-ray diffraction with four-circle goniometers from 20° to 60° in steps of 0.05°. The x-ray diffraction pattern showed very sharp (00 l) peaks. Figure 1 shows the low-field magnetization at 10 Oe and the transition temperature T_c was found to be 27 K. The value of the zero-field-cooled (ZFC) $4\pi M/H$ is about 2 due to a demagnetization factor. The high-field magnetization experiment was carried out using a SQUID magnetometer (MPMS, Quantum Design, Inc.) for fields applied parallel to the c axis. The ZFC and field-cooled (FC) magnetizations for the external field range of $0.1 \text{ T} \leq H \leq 1.2 \text{ T}$ were measured: The magnetization data above this range were not reliable, because noise became larger.

III. RESULTS AND DISCUSSION

Figure 2 shows the temperature dependence of the reversible magnetization $4\pi M(T)$ for fields up to 1.2 T along the c axis. The inset of Fig. 2 shows $M(T)$ in the temperature range from 21 to 27 K. A prominent feature is that the magnetization curves for different fields cross at $T^* = 25.3$ K with a value of $4\pi M(T^*) = -1.52$ G, which has been known for

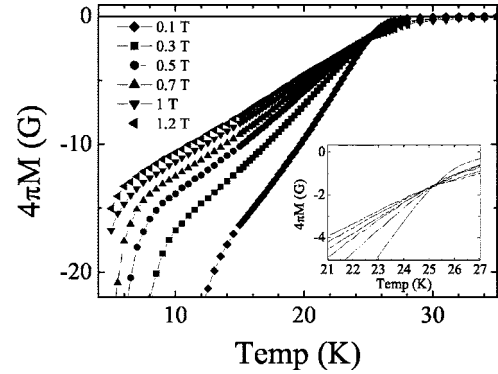


FIG. 2. Temperature dependence of the reversible magnetization in the field range of $0.1 \text{ T} \leq H \leq 1.2 \text{ T}$. The inset shows $M(T)$ curves near $T_c(H)$.

the clear evidence of the positional fluctuations of vortices.¹¹ This is a typical behavior for highly anisotropic layered superconductors with a strong fluctuation effect.^{12–17}

Thermal fluctuations cause the magnetization curve to deviate from that predicted by the mean-field theory.¹⁸ As a result, in the Hao-Clem model based on the Ginzburg-Landau theory, $\kappa(T)$ increases unphysically near T_c . However, far away from T_c , the effects of thermal fluctuations are less important, so we can apply the Hao-Clem model to $M(T)$.¹⁹ In the Hao-Clem model, not only the electromagnetic energy outside of the vortex core, but also the core energy arising from the suppression of the order parameter at the vortex core are included. By using this model, the reversible magnetization can be calculated and obtained thermodynamic parameters like H_c .

In the Hao-Clem model, the reversible magnetization in dimensionless form $-4\pi M'$ is a universal function for a given value of the GL parameter κ and is temperature independent. Here the magnetization and external field are defined as $-4\pi M' = -4\pi M / \sqrt{2}H_c(T)$ and $H' = H / \sqrt{2}H_c(T)$.¹⁹ At a fixed temperature, the ratio $-4\pi M_i(H_i) / H_i$ ($i=1, 2, \dots$) in experimental data corresponds to the ratio $-4\pi M' / H'$ at a certain point on the theoretical curve with a given κ . By means of this correspondence, the value of $\sqrt{2}H_c(T)$ is determined from the ratio H' / H_i for each $i=1, 2, \dots$. If the value of κ is appropriately selected, then it results in the smallest error in $\sqrt{2}H_c(T)$.

From this procedure, $\kappa(T)$ and $H_c(T)$ are obtained in the temperature range of $14.5 \text{ K} \leq T \leq 20 \text{ K}$ with the average value $\kappa_{av} = 89$ as shown in Fig. 3(a). However, an anomalous increase starts from $T \approx 0.74T_c$. As mentioned above, this unphysical rapid increase can be understood to originate from fluctuation effects. In contrast to 2D superconductors, in three-dimensional (3D) superconductors, thermal fluctuations are less pronounced, and $\kappa(T)$ starts to increase very near T_c .^{20–22} With this κ value, $-4\pi M(H)$ curves could be scaled to one universal curve, consistent with the Hao-Clem model. The inset of Fig. 3(a) shows $-4\pi M'$ versus H' for the experimental data and the theoretical fitting. All the data clearly collapse onto a single curve.

Figure 3(b) shows the temperature dependence of H_c . The solid line represents the two-fluid model for H_c , which yields

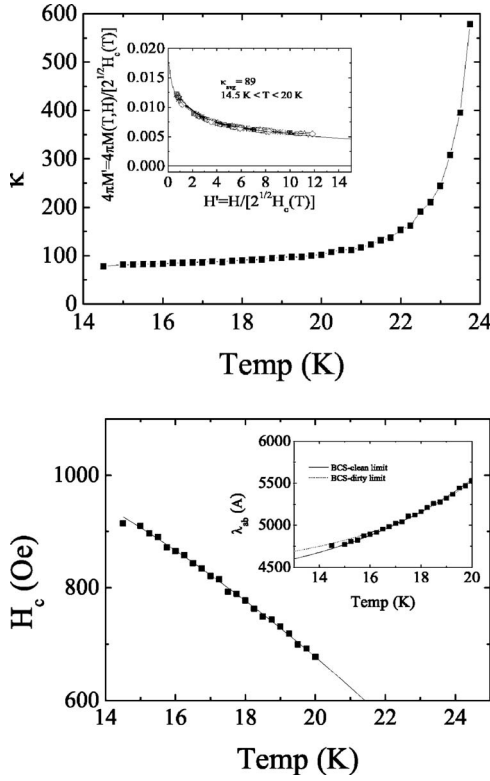


FIG. 3. (a) Temperature dependence of $\kappa(T)$ extracted from the Hao-Clem model. The inset shows the magnetization $-4\pi M' = -4\pi M/\sqrt{2}H_c(T)$ vs $H' = H/\sqrt{2}H_c(T)$. The solid line represents the universal curve derived from the model of Hao *et al.* with $\kappa=89.0$. (b) Temperature dependence of H_c . The solid line represents the two-fluid model, which yields $H_c(0)=1202.3$ Oe and $T_c=30.2$ K. The inset shows the temperature dependence of the penetration depth $\lambda_{ab}(T)$ obtained from the Hao-Clem model. The solid and the dashed lines represent the BCS clean and dirty limits, respectively.

$H_c(0)=0.12$ T and $T_c=26.5$ K. Once $H_c(T)$ and κ were obtained, we calculated several thermodynamic parameters. According to the relation $H_{c2}(T)=\sqrt{2}\kappa H_c(T)$, the value of the upper critical field slope, $(dH_{c2}/dT)_{T_c}$ was estimated to be -0.87 T/K. This slope can be used to calculate the upper critical field at $T=0$ by using the Werthamer-Helfand-Hohenberg formula.²³ From this formula, $H_{c2}(0)$ is estimated to be 16.9 T in the clean limit and 16.1 T in the dirty limit, which correspond to $\xi_{ab}(0)=44.1$ Å and $\xi_{ab}(0)=45.2$ Å, respectively, according to the relation of $H_{c2}(0)=\phi_0/2\pi\xi_{ab}^2$. The penetration depth $\lambda(T)$, as shown in the inset of Fig. 3(b), was evaluated by using the relationship $\lambda = \kappa(\phi_0/2\pi H_{c2})^{1/2}$. The solid and dashed lines represent the BCS clean and dirty limits for $\lambda(T)$, respectively. From this analysis, $\lambda_{ab}(0)$ is estimated to be 4380 Å for the clean limit and 4530 Å for the dirty limit. The total error of the above superconducting parameters is estimated to be less than 10%. Table I summarizes the superconducting parameters of $\text{Ca}_{1.82}\text{Na}_{0.18}\text{CuO}_2\text{Cl}_2$ as well as those of $\text{La}_{1.82}\text{Sr}_{0.18}\text{CuO}_4$ (Refs. 24–26) and Bi-2212.²⁷ Quite unexpectedly, $\lambda_{ab}(0)$ for $\text{Ca}_{1.82}\text{Na}_{0.18}\text{CuO}_2\text{Cl}_2$ is considerably larger than that for $\text{La}_{1.82}\text{Sr}_{0.18}\text{CuO}_4$. This is due to either the decrease of the superfluid density n_s or the increase of the effective mass m^*

TABLE I. Thermodynamic properties of $\text{Ca}_{1.82}\text{Na}_{0.18}\text{CuO}_2\text{Cl}_2$ (Na-CCOC), $\text{La}_{1.82}\text{Sr}_{0.18}\text{CuO}_4$ (LSCO) (Ref. 24), and $\text{Bi}_2\text{Sr}_2\text{CaCu}_2\text{O}_{8-\delta}$ (Bi-2212) (Ref. 27).

	T_c^{onset} (K)	κ	$H_c(0)$ (Oe)	$H_{c2}(0)$ (T)	$\lambda_{ab}(0)$ (Å)	ξ_{ab} (Å)
Na-CCOC	27	89.0	1202	16.9	4380	44.1
LSCO	30	75	2170	21	2380	33
Bi-2212	85	266	9753	156	2438	9.5

because $\lambda_{ab}^{-2} \propto n_s/m^*$. However, the latter is improbable because m^* was reported to be constant irrespective of the doping in YBCO and LSCO. Therefore, the increase in $\lambda_{ab}(0)$ is thought to originate mainly from the decrease in n_s . The n_s of Na-CCOC is much smaller than that of iso-structural superconductor $\text{La}_{1.82}\text{Sr}_{0.18}\text{CuO}_4$. The $\lambda_{ab}(0)$ is even larger than that for Bi-2212.

The anisotropic nature of the Na-CCOC crystal could be deduced once we had investigated the scaling behavior of the fluctuation-induced magnetization in the high-field region. According to Ullah and Dorsey,¹⁰ in the critical region near T_c , the scaling form for the magnetization is given by

$$\frac{4\pi M}{(TH)^n} = F \left[A \frac{T - T_c(H)}{(TH)^n} \right], \quad (1)$$

where F is a scaling function. A is a temperature and field independent coefficient, and the exponent n is 2/3 for 3D and 1/2 for 2D. The magnetization scaled by using the 2D scaling form is shown in Fig. 4. For each field, all data collapse onto a single curve, consistent with the 2D nature of the Na-CCOC crystal. This analysis provides $T_c=27.1$ K and the slope $dH_{c2}/dT_c=-0.8$ T/K near T_c , which are very close to the values derived from the Hao-Clem model. We checked the 3D scaling, but in this case, the $M(T)$ curves did not collapse onto a universal curve. It should be noted that the fluctuation-induced magnetization for $\text{La}_{1.82}\text{Sr}_{0.18}\text{CuO}_4$ follows a 3D scaling behavior.²⁸

Another indication of the 2D nature of Na-CCOC is seen in the irreversibility line H_{irr} . Figure 5 shows the irreversibility line H_{irr} of Na-CCOC (open circles) obtained from the magnetization for $0.01 \leq H \leq 1.2$ T. The irreversibility temperature, T_{irr} , was determined from the simple criterion $M_{fc}/M_{zfc}=0.98$. For comparison, the values of H_{irr} for

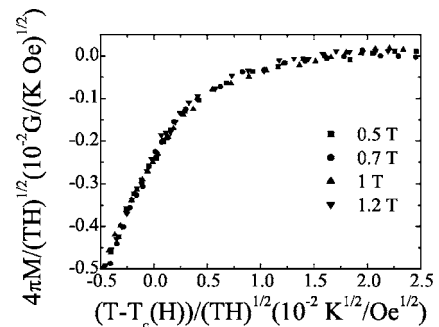


FIG. 4. 2D scaling of the magnetization around $T_c(H)$.

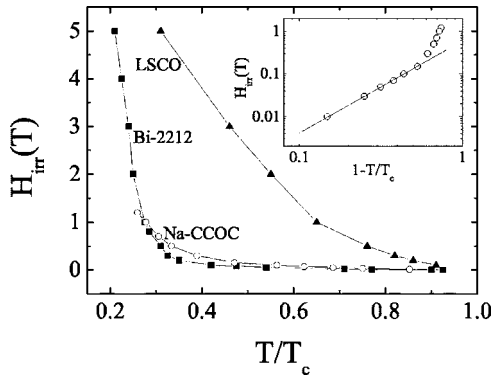


FIG. 5. Irreversibility lines of $\text{Ca}_{1.82}\text{Na}_{0.18}\text{CuO}_2\text{Cl}_2$, $\text{La}_{1.82}\text{Sr}_{0.18}\text{CuO}_4$, and $\text{Bi}_2\text{Sr}_2\text{CaCu}_2\text{O}_8$. The inset shows a log-log plot of H_{irr} vs $1-T/T_c$. The solid line is the fitting curve $H_{irr}(T) = H_0(1-T/T_c)^n$.

LSCO and Bi-2212 crystals are plotted in the same figure.²⁹ We note that H_{irr} for Na-CCOC is comparable with that for Bi-2212. The inset of Fig. 5 shows a log-log plot of H_{irr} versus $1-T/T_c$. H_{irr} is linear at high temperature in this plot; i.e., H_{irr} has a power-law behavior. The solid line represents $H_{irr} = H_0(1-T/T_c)^n$ below $H = 0.15$ T. We can obtain the $H_0 = 0.59$ T and $n = 2.16$. For Bi-2212 and LSCO, the values of n are about 2 and 1.5, respectively.²⁹ In the frame work of the vortex fluctuation model,^{29,30} H_0 can be expressed as

$$H_0 = \frac{\phi_0^5 c_L^4}{16\pi^3 \lambda_{ab}^4(0) \gamma^2 k_B^2 T_c^2}, \quad (2)$$

where ϕ_0 is the flux quantum and c_L is the Lindemann number.³¹ c_L^2/γ is estimated to be 2.0×10^{-4} for $\lambda_{ab}(0) = 438$ nm. If we use the value of $0.1 \leq c_L \leq 0.4$, γ of Na-CCOC lies in the range $50.3 \leq \gamma \leq 804$. This range of γ seems to be comparable to or larger than that for Bi-2212 ($\gamma \sim 55$),³² and much larger than that for LSCO ($10 \leq \gamma \leq 25$).²⁵ These results indicate that the Na-CCOC crystal is

much more anisotropic than LSCO and are consistent with the conclusion deduced from the optical conductivity spectra.³³

IV. SUMMARY

The reversible magnetization for a high-quality $\text{Ca}_{1.82}\text{Na}_{0.18}\text{CuO}_2\text{Cl}_2$ single crystal with $T_c = 27$ K was measured with the magnetic field along the c direction. The $M(T)$ data show a crossover of the magnetization at $T^* = 25.3$ K, which indicates a strong vortex fluctuation effect. By applying the Hao-Clem model to the experimental $M(T)$, we obtained several thermodynamic parameters. Surprisingly, the superconducting parameters show behaviors quite different from those for $\text{La}_{1.82}\text{Sr}_{0.18}\text{CuO}_4$. For example, $\lambda_{ab}(0)$ is estimated to be 4380 Å in the clean limit, which is almost twice the value for $\text{La}_{1.82}\text{Sr}_{0.18}\text{CuO}_4$. In addition, unlike $\text{La}_{1.82}\text{Sr}_{0.18}\text{CuO}_4$, the fluctuation-induced magnetization and the irreversibility line for $\text{Ca}_{1.82}\text{Na}_{0.18}\text{CuO}_2\text{Cl}_2$ show pronounced two-dimensional behaviors. These results lead us to the conclusion that despite their having the same structure with the replacement of apical atoms, drastic differences are observed between the superconducting properties of $\text{Ca}_{1.82}\text{Na}_{0.18}\text{CuO}_2\text{Cl}_2$ and $\text{La}_{1.82}\text{Sr}_{0.18}\text{CuO}_4$ single crystals. This is thought to be caused because chlorine at the apical site is less effective than oxygen in supplying the charge carriers to CuO_2 planes and as a result, the interlayer coupling between the CuO_2 planes is weakened. Our conclusion is consistent with theoretical³⁴ and experimental³⁵ studies which indicates that the bonding between Cu $3d$ and Cl $3p$ orbitals is much weaker than that between Cu $3d$ and O $2p$ orbitals.

ACKNOWLEDGMENT

This work was supported by the Ministry of Science and Technology of Korea through the Creative Research Initiative Program.

¹Z. Hiroi, N. Kobayashi, and M. Takano, *Nature (London)* **371**, 139 (1994).

²Y. Kohsaka, M. Azuma, I. Yamada, T. Sasagawa, T. Hanaguri, M. Takano, and H. Takagi, *J. Am. Chem. Soc.* **124**, 12275 (2002).

³T. Hanaguri, C. Lupien, Y. Kohsaka, D.-H. Lee, M. Azuma, M. Takano, H. Takagi, and J. C. Davis, *Nature (London)* **430**, 1001 (2004).

⁴K. McElroy, D.-H. Lee, J. E. Hoffman, K. M. Lang, J. Lee, E. W. Hudson, H. Eisaki, S. Uchida, and J. C. Davis, *cond-mat/0406491*.

⁵F. Ronning, C. Kim, Y. D. L. Feng, D. S. Marshall, A. G. Loeser, L. L. Miller, J. N. Eckstein, I. Bozovic, and Z.-X. Shen, *Science* **282**, 2067 (1998).

⁶F. Ronning, T. Sasagawa, Y. Kohsaka, K. M. Shen, A. Damascelli, C. Kim, T. Yoshida, N. P. Armitage, D. H. Lu, D. L. Feng, L. L. Miller, H. Takagi, and Z.-X. Shen, *Phys. Rev. B* **67**, 165101 (2003).

⁷Y. Kohsaka, T. Sasagawa, F. Ronning, T. Yoshida, C. Kim, T. Hanaguri, M. Azuma, M. Takano, Z.-X. Shen, and H. Takagi, *J. Phys. Soc. Jpn.* **72**, 1018 (2003).

⁸A. Ino, C. Kim, M. Nakamura, T. Yoshida, T. Mizokawa, Z.-X. Shen, A. Fujimori, T. Kakeshita, H. Eisaki, and S. Uchida, *Phys. Rev. B* **62**, 4137 (2000).

⁹Z. Hiroi, N. Kobayashi, and M. Takano, *Physica C* **266**, 191 (1996).

¹⁰S. Ullah and A. T. Dorsey, *Phys. Rev. Lett.* **65**, 2066 (1990).

¹¹L. N. Bulaevskii, M. Ledvij, and V. G. Kogan, *Phys. Rev. Lett.* **68**, 3773 (1992).

¹²Mun-Seog Kim, C. U. Jung, Sung-Ik Lee, and A. Iyo, *Phys. Rev. B* **63**, 134513 (2001).

¹³Mun-Seog Kim, Sung-Ik Lee, Seong-Cho Yu, and Nam H. Hur, *Phys. Rev. B* **53**, 9460 (1996).

¹⁴Myoung-Kwang Bae, Mun-Seog Kim, Sung-Ik Lee, Nam-Gyu Park, Seong-Ju Hwang, Dong-Hoon Kim, and Jin-Ho Choy,

- Phys. Rev. B **53**, 12416 (1996).
- ¹⁵A. Wahl, V. Hardy, F. Warmont, A. Maignan, M. P. Delamare, and Ch. Simon, Phys. Rev. B **55**, 3929 (1997).
- ¹⁶Heon-Jung Kim, P. Chowdhury, In-Sun Jo, and Sung-Ik Lee, Phys. Rev. B **66**, 134508 (2002).
- ¹⁷Kyung-Hee Kim, Heon-Jung Kim, Sung-Ik Lee, A. Iyo, Y. Tanaka, K. Tokiwa, and T. Watanabe, Phys. Rev. B **70**, 092501 (2004).
- ¹⁸V. G. Kogan, M. Ledvij, A. Yu. Simonov, J. H. Cho, and D. C. Johnston, Phys. Rev. Lett. **70**, 1870 (1993).
- ¹⁹Z. Hao and J. R. Clem, Phys. Rev. Lett. **67**, 2371 (1991); Zhi-dong Hao, John R. Clem, M. W. McElfresh, L. Civale, A. P. Malozemoff, and F. Holtzberg, Phys. Rev. B **43**, 2844 (1991).
- ²⁰Mun-Seog Kim, Sung-Ik Lee, A. Iyo, K. Tokiwa, M. Tokumoto, and H. Ihara, Phys. Rev. B **57**, 8667 (1998).
- ²¹Junho Gohng and D. K. Finnemore, Phys. Rev. B **46**, 398 (1992).
- ²²Junghyun Sok, Ming Xu, Wei Chen, B. J. Suh, J. Gohng, D. K. Finnemore, M. J. Kramer, L. A. Schwartzkopf, and B. Dabrowski, Phys. Rev. B **51**, 6035 (1995).
- ²³N. R. Werthamer, E. Helfand, and P. C. Hohenberg, Phys. Rev. **147**, 295 (1966).
- ²⁴Qiang Li, M. Suenaga, T. Kimura, and K. Kishio, Phys. Rev. B **47**, 11384 (1993).
- ²⁵T. Shibauchi, H. Kitano, K. Uchinokura, A. Maeda, T. Kimura, and K. Kishio, Phys. Rev. Lett. **72**, 2263 (1994).
- ²⁶A. J. Zaleski and J. Klamut, Phys. Rev. B **59**, 14023 (1999).
- ²⁷H.-C. Ri, R. Gross, F. Gollnik, A. Beck, R. P. Huebener, P. Wagner, and H. Adrian, Phys. Rev. B **50**, 3312 (1994).
- ²⁸H. Iwasaki, F. Matsuoka, and K. Tanigawa, Phys. Rev. B **59**, 14624 (1999).
- ²⁹A. Schilling, R. Jin, J. D. Guo, and H. R. Ott, Phys. Rev. Lett. **71**, 1899 (1993).
- ³⁰A. Schilling, M. Cantoni, J. D. Guo, and H. R. Ott, Nature (London) **363**, 56 (1993).
- ³¹A. Houghton, R. A. Pelcovits, and A. Sudbø, Phys. Rev. B **40**, 6763 (1989).
- ³²D. E. Farrell, B. S. Chandrasekhar, M. R. DeGuire, M. M. Fang, V. G. Kogan, J. R. Clem, and D. K. Finnemore, Phys. Rev. B **36**, 4025 (1987).
- ³³K. Waku, T. Katsufuji, Y. Kohsaka, T. Sasagawa, H. Takagi, H. Kishida, H. Okamoto, M. Azuma, and M. Takano, Phys. Rev. B **70**, 134501 (2004).
- ³⁴L. F. Mattheiss, Phys. Rev. B **42**, 354 (1990).
- ³⁵A. Fujimori, Y. Tokura, H. Eisaki, H. Takagi, S. Uchida, and M. Sato, Phys. Rev. B **40**, 7303 (1989).